

# Non-Gaussianity from resonant curvaton decay

Alex Chambers<sup>a</sup>, Sami Nurmi<sup>b</sup> and Arttu Rajantie<sup>a</sup>

<sup>a</sup> Department of Physics, Imperial College London, London SW7 2AZ, United Kingdom

<sup>b</sup>Institute for Theoretical Physics, University of Heidelberg, 69120 Heidelberg, Germany

E-mail: alex.chambers05@imperial.ac.uk, s.nurmi@thphys.uni-heidelberg.de and a.rajantie@imperial.ac.uk

**Abstract.** We calculate curvature perturbations in the scenario in which the curvaton field decays into another scalar field via parametric resonance. As a result of a nonlinear stage at the end of the resonance, standard perturbative calculation techniques fail in this case. Instead, we use lattice field theory simulations and the separate universe approximation to calculate the curvature perturbation as a nonlinear function of the curvaton field. For the parameters tested, the generated perturbations are highly non-Gaussian and not well approximated by the usual  $f_{\text{NL}}$  parameterisation. Resonant decay plays an important role in the curvaton scenario and can have a substantial effect on the resulting perturbations.

PACS numbers: 98.80.Cq, 11.15.Kc

## 1. Introduction

Observations of the cosmic microwave background radiation are consistent with Gaussian perturbations [1], but there are tantalising hints of non-Gaussianity [2] at a level that would be clearly observable with the Planck satellite and other future experiments [3]. This would rule out the simplest inflationary models with slowly rolling scalar fields, which can only produce very-nearly-Gaussian perturbations [4–7].

Models which can generate large non-Gaussianities either during, or at the end of, inflation include those with non-canonical Lagrangians [8–16], those where there is breakdown of slow-roll dynamics during inflation due to sharp features in the potential [17, 18], those with multiple fields with specific inflationary trajectories in the field space [19–27] and those where additional light scalars affect the dynamics of perturbative or non-perturbative inflaton decay [28–39].

A well-known example of a multi-field model where large non-Gaussianities can be generated after the end of inflation is the curvaton scenario [40–44]. In this model, the primordial perturbations arise from the curvaton field, a scalar field which is light relative to the Hubble rate during inflation but, unlike the inflaton, gives a subdominant contribution to the energy density.

After inflation the relative curvaton contribution to the total energy density increases. This affects the expansion of space, and the curvaton perturbations become imprinted on the metric fluctuations. The standard adiabatic hot big bang era is recovered when the curvaton eventually decays and thermalises with the existing radiation. The mechanism can be seen as a conversion of initial isocurvature perturbations into adiabatic curvature perturbations during the post-inflationary epoch. If the curvaton remains subdominant even at the time of its decay, its perturbations need to be relatively large to yield the observed amplitude of primordial perturbations. Consequently, in this limit the curvaton scenario typically generates significant non-Gaussianities [45–52].

Almost all the analysis of the curvaton scenario is based on the assumption of a perturbative curvaton decay. As pointed out in refs. [53, 54], it is, however, possible that the curvaton decays through a non-perturbative process analogous to inflationary preheating [55–57]. This is a natural outcome in models where the curvaton is coupled to other scalar fields which acquire effective masses proportional to the value of the curvaton field.

During this short period of non-equilibrium physics, part of the curvaton condensate decays rapidly into quanta of other light scalar fields. In analogy to inflationary preheating, the decay is not complete and the remaining curvaton particles have to decay perturbatively. The properties of primordial perturbations generated in the curvaton scenario depend sensitively on the dynamics after the end of inflation until the time of the curvaton decay [58–60]. As the preheating dynamics are highly nonlinear, it is natural to ask if this stage could generate large non-Gaussianities.

Our aim in this work is to calculate the amplitude and non-Gaussianity of perturbations from curvaton preheating. To do this we use the separate universe approximation [61–64] and classical lattice field theory simulations [65, 66]. This method was applied to inflationary preheating in refs. [37–39]. We solve coupled field and Friedmann equations to determine the expansion of the universe during the non-equilibrium dynamics and the fraction of the curvaton energy which is converted into radiation. From these, we calculate the curvature perturbation as a function of the local value of the curvaton field. We find that, at least for our choice of parameters, this dependence is highly nonlinear, implying very high levels of non-Gaussianity.

The structure of the paper is as follows. In section 2 we review the curvaton model and derive useful general results. In section 3 we present an analytic calculation of production of curvature perturbations using linearised approximation of preheating dynamics, and demonstrate that the answers depend on quantities that are not calculable in linear theory. A full nonlinear computation is, therefore, needed. In section 4 we show how this can be done, and compute the amplitude and non-Gaussianity of the perturbations for three sets of parameters. Finally, we present our conclusions in section 5.

## 2. General theory

### 2.1. Model

We study the curvature perturbations generated in a simple curvaton model with canonical kinetic terms and the potential

$$V(\phi, \sigma, \chi) = V(\phi) + \frac{1}{2}m^2\sigma^2 + \frac{1}{2}g^2\sigma^2\chi^2, \quad (1)$$

where  $\phi$  is the inflaton,  $\sigma$  is the curvaton and  $\chi$  is a scalar field which the curvaton will decay into. During inflation the inflaton potential  $V(\phi)$  dominates the energy density. We assume standard slow roll inflation, so the inflaton field rolls down its potential until it reaches a critical value  $\phi_*$  at which the slow roll conditions fail and inflation ends. As usual, the perturbations of the inflaton field generate curvature perturbations, but we assume that their amplitude is negligible. This requires  $H/\sqrt{\epsilon} \ll 10^{-5}$ , where  $H$  is the Hubble rate and  $\epsilon$  is the slow roll parameter, both of which are determined by the inflaton potential  $V(\phi)$ .

Instead, we assume that the observed primordial perturbations are generated solely by the curvaton field  $\sigma$ , which should be light during inflation so that it develops nearly scale-invariant quantum fluctuations similar to those of the inflaton field. The curvaton field remains nearly frozen at the value  $\sigma_*$  it had at the end of inflation, until the time  $t_{\text{osc}}$  at which the Hubble parameter has decreased to  $H \sim m$  and the curvaton starts to oscillate around the minimum of its potential. These fluctuations contribute to the energy density, and, therefore, they affect the expansion of the universe and generate curvature perturbations.

Eventually, the curvaton  $\sigma$  decays into lighter degrees of freedom. In the standard curvaton scenario this decay is assumed to take place perturbatively. The interaction term in (1) only allows pair annihilations, the rate of which falls quickly when the universe expands. Some of the curvaton particles would, therefore, survive until today, behaving as dark matter. While this might be an interesting scenario to study, we follow most of the literature and assume that the curvaton is also coupled to other fields. In particular, a Yukawa coupling to a light (possibly Standard Model) fermion field  $\psi$  of the form

$$\mathcal{L}_{\text{Yukawa}} = h\sigma\bar{\psi}\psi \quad (2)$$

would give the decay rate [57]

$$\Gamma = \frac{h^2 m}{8\pi}. \quad (3)$$

Without further knowledge of the curvaton couplings, the decay rate  $\Gamma$  appears as a free phenomenological parameter, which is bounded from below because the curvaton cannot decay arbitrarily late without spoiling the success of the hot big bang cosmology. The most conservative lower bound for the decay time is given by nucleosynthesis:  $\Gamma \gtrsim T_{\text{BBN}}^2/M_{\text{Pl}}$  [67].

In this work, we assume that the other scalar field  $\chi$  in (1) is heavy during inflation,  $g\sigma \gtrsim H$ , so that its value remains close to zero and it develops no long-range perturbations. It was recently shown in ref. [54] that in this case some of the curvaton particles can decay via a parametric resonance into quanta of the  $\chi$  field. The resonance does not destroy all the curvaton particles, so a Yukawa coupling is still needed to allow those which remain to decay perturbatively. However, it reduces their density significantly.

## 2.2. Curvature perturbations

Using the  $\delta N$  approach, the curvature perturbation  $\zeta$  on superhorizon scales is given by the expression [62]

$$\zeta = \delta \ln a \Big|_{\rho}, \quad (4)$$

where  $a|_{\rho}$  is the scale factor at some fixed energy density  $\rho$ , and  $\delta$  denotes the difference from the mean value over the whole currently observable universe. The scale factor  $a$  is normalised to be constant at some earlier flat hypersurface, which we choose to be at the end of inflation. This measures the difference in the integrated expansion between Friedmann–Robertson–Walker (FRW) solutions with different initial conditions which are evolved until the same final energy density  $\rho$ . In our case, the variations of initial conditions arise from the super-horizon fluctuations of the curvaton field  $\delta\sigma_*$  produced during inflation. This means that the curvature perturbation is a local function of the curvaton field fluctuations  $\zeta = \zeta(\delta\sigma_*)$ . As we know the statistics of  $\delta\sigma_*$ , this determines the statistics of the curvature perturbation  $\zeta$  completely. In this paper we compute this function.

Observations show that the primordial perturbations were nearly Gaussian, which implies that  $\zeta(\delta\sigma_*)$  should be approximately linear. Therefore, it is natural to Taylor expand (4) as

$$\zeta = (\ln a)' \Big|_{\rho} \delta\sigma_* + \frac{1}{2} (\ln a)'' \Big|_{\rho} \delta\sigma_*^2 + \dots, \quad (5)$$

where the prime denotes a partial derivative with respect to the curvaton value at the end of inflation  $\sigma_*$  evaluated at constant final energy density  $\rho$ . This implies that, to leading order in  $\delta\sigma_*$ , the power spectrum of the curvature perturbations is

$$\mathcal{P}_{\zeta}(k) = \left[ (\ln a)' \Big|_{\rho} \right]^2 \mathcal{P}_{\sigma}(k), \quad (6)$$

where  $\mathcal{P}_{\sigma}(k)$  is the power spectrum of the curvaton field. Assuming the curvaton perturbations at the end of inflation  $\delta\sigma_*$  are Gaussian, the expansion (5) is of the form [68]

$$\zeta = \zeta_g + \frac{3}{5} f_{\text{NL}} \zeta_g^2 + \dots, \quad (7)$$

where  $\zeta_g$  is a Gaussian field and  $f_{\text{NL}}$  is a position independent constant. This defines the local nonlinearity parameter  $f_{\text{NL}}$  and, according to (5), the  $\delta N$  formalism gives [69]

$$f_{\text{NL}} = \left. \frac{5}{6} \frac{(\ln a)''}{(\ln a)'^2} \right|_{\rho}. \quad (8)$$

Neglecting the inherent non-Gaussianity of the curvaton perturbations  $\delta\sigma_*$  yields an error proportional to slow-roll parameters. This is irrelevant in the limit  $|f_{\text{NL}}| \gg 1$ , which is the main focus of this work. The WMAP data and other recent observations give the constraint  $|f_{\text{NL}}| \lesssim 100$  [1–3, 70].

In this paper we focus on the case in which the curvaton field decays into  $\chi$  particles through a parametric resonance, at the end of which the fields undergo a period of potentially very complicated, nonlinear, non-equilibrium dynamics. Afterwards, the fields equilibrate, and we assume that eventually the universe behaves as a mixture of non-interacting matter and radiation. This assumption is checked using simulations in section 4 and we find it to be accurate enough for our current purposes. Therefore, we parameterise the total energy density as a sum of matter and radiation components

$$\rho = \rho_{\text{ref}} \left[ r_{\text{ref}} \left( \frac{a_{\text{ref}}}{a} \right)^3 + (1 - r_{\text{ref}}) \left( \frac{a_{\text{ref}}}{a} \right)^4 \right], \quad (9)$$

where  $a_{\text{ref}}$ ,  $\rho_{\text{ref}}$  and  $r_{\text{ref}} = \rho_{m,\text{ref}}/\rho_{\text{ref}}$  are the scale factor, energy density and matter fraction at some arbitrary reference time well after the resonance is over.‡

We assume that the inflaton field has either decayed into ultrarelativistic degrees of freedom or is itself ultrarelativistic, so that it contributes to the radiation component. The  $\chi$  field is also ultrarelativistic; the only degree of freedom that contributes to the matter component is the curvaton.

If the resonance destroyed all of the curvaton particles,  $r_{\text{ref}}$  would be zero, but, in practice, some curvatons are left over. We assume  $r_{\text{ref}} \ll 1$  which corresponds to the curvaton being subdominant at the end of the resonance. We can then rearrange (9) to give, at leading order in  $r_{\text{ref}}$ , the scale factor at energy density  $\rho$

$$\ln a = \ln a_{\text{ref}} + \frac{1}{4} \left[ \ln \frac{\rho_{\text{ref}}}{\rho} + r_{\text{ref}} \left( \left( \frac{\rho_{\text{ref}}}{\rho} \right)^{1/4} - 1 \right) \right], \quad (10)$$

where we have assumed that the curvaton is still subdominant at this time. That is

$$r \equiv r_{\text{ref}} \left( \frac{\rho_{\text{ref}}}{\rho} \right)^{1/4} \ll 1. \quad (11)$$

The curvature perturbation is given by combining (4) with (10). In general,  $a_{\text{ref}}$ ,  $\rho_{\text{ref}}$  and  $r_{\text{ref}}$  all vary between one separate universe and another. In our case, the variation is entirely due to fluctuations of  $\sigma_*$ , the value of the curvaton field during inflation. In order to calculate the curvature perturbation using (5) we differentiate (10) with respect

‡ We define  $r = \rho_m/\rho$  following ref. [43]. This differs from the variable  $r$  used in ref. [45] by a factor of 3/4 in the limit  $r \ll 1$ .

to  $\sigma_*$  keeping the final energy density  $\rho$  fixed. This gives

$$\begin{aligned} (\ln a)' \Big|_{\rho} &= (\ln a_{\text{ref}})' + \frac{1}{4} \left[ \frac{\rho'_{\text{ref}}}{\rho_{\text{ref}}} + r_{\text{ref}} \frac{\rho'_{\text{ref}}}{4\rho^{1/4}\rho_{\text{ref}}^{3/4}} + r'_{\text{ref}} \left( \left( \frac{\rho_{\text{ref}}}{\rho} \right)^{1/4} - 1 \right) \right] \\ &= (\ln a_{\text{ref}})' + \frac{1}{4} \left[ \left( 1 + \frac{r}{4} \right) \frac{\rho'_{\text{ref}}}{\rho_{\text{ref}}} + (r - r_{\text{ref}}) \frac{r'_{\text{ref}}}{r_{\text{ref}}} \right], \end{aligned} \quad (12)$$

$$\begin{aligned} (\ln a)'' \Big|_{\rho} &= (\ln a_{\text{ref}})'' + \frac{1}{4} \left[ \frac{\rho''_{\text{ref}}}{\rho_{\text{ref}}} - \left( \frac{\rho'_{\text{ref}}}{\rho_{\text{ref}}} \right)^2 + \frac{r_{\text{ref}}}{4} \left( \frac{\rho_{\text{ref}}}{\rho} \right)^{1/4} \left( \frac{\rho''_{\text{ref}}}{\rho_{\text{ref}}} - \frac{3}{4} \left( \frac{\rho'_{\text{ref}}}{\rho_{\text{ref}}} \right)^2 \right) \right. \\ &\quad \left. + r'_{\text{ref}} \frac{\rho'_{\text{ref}}}{2\rho^{1/4}\rho_{\text{ref}}^{3/4}} + r''_{\text{ref}} \left( \left( \frac{\rho_{\text{ref}}}{\rho} \right)^{1/4} - 1 \right) \right] \\ &= (\ln a_{\text{ref}})'' + \frac{1}{4} \left[ \frac{\rho''_{\text{ref}}}{\rho_{\text{ref}}} - \left( \frac{\rho'_{\text{ref}}}{\rho_{\text{ref}}} \right)^2 + \frac{r}{4} \left( \frac{\rho''_{\text{ref}}}{\rho_{\text{ref}}} - \frac{3}{4} \left( \frac{\rho'_{\text{ref}}}{\rho_{\text{ref}}} \right)^2 \right) \right. \\ &\quad \left. + \frac{r}{2} \frac{r'_{\text{ref}}}{r_{\text{ref}}} \frac{\rho'_{\text{ref}}}{\rho_{\text{ref}}} + (r - r_{\text{ref}}) \frac{r''_{\text{ref}}}{r_{\text{ref}}} \right]. \end{aligned} \quad (13)$$

The remaining curvatons decay within a fixed time  $1/\Gamma$  where the decay rate  $\Gamma$  depends on the curvaton interactions. We assume that all matter in the universe is ultrarelativistic after the curvaton decay, so that the universe becomes radiation dominated and evolves adiabatically. Following the sudden decay approximation [43], we assume that this decay takes place instantaneously at a fixed energy density  $\rho_{\text{decay}}$ , which is determined by the curvaton decay rate  $\Gamma$ . The final curvature perturbation is therefore given by setting  $\rho = \rho_{\text{decay}}$  in (12) and (13), or equivalently  $r = r_{\text{decay}}$ , where

$$r_{\text{decay}} = r_{\text{ref}} \left( \frac{\rho_{\text{ref}}}{\rho_{\text{decay}}} \right)^{1/4}. \quad (14)$$

The decay rate  $\Gamma$  is unknown, so we can treat  $r_{\text{decay}}$  as a free parameter.

### 2.3. Standard perturbative decay

As a simple example of the calculation of perturbations, and to aid comparison with our results for resonant curvaton decay, we first summarise the standard perturbative calculation of perturbations generated in the curvaton model [43, 45].

This calculation ignores the resonance, so (9) is assumed to be valid from the start of the curvaton oscillations, which we can therefore choose as our reference time,  $t_{\text{ref}} = t_{\text{osc}}$ . This time is determined by the condition  $H \approx m$ , which implies that  $\rho_{\text{ref}} = \rho_{\text{osc}} \approx m^2 M_{\text{Pl}}^2$  independently of  $\sigma_*$ . Furthermore, the scale factor  $a_{\text{ref}} = a_{\text{osc}}$  is also independent of  $\sigma_*$  to good approximation, because the curvaton contribution to the energy density is negligible during inflation. Perturbations are therefore generated solely by derivatives of  $r_{\text{ref}} = r_{\text{osc}}$ , the matter fraction at the start of the oscillations, and (12) and (13) simplify to

$$(\ln a)' \Big|_{\rho} = \frac{r_{\text{decay}}}{4} \frac{r'_{\text{osc}}}{r_{\text{osc}}}, \quad (15)$$

$$(\ln a)'' \Big|_{\rho} = \frac{r_{\text{decay}}}{4} \frac{r''_{\text{osc}}}{r_{\text{osc}}}, \quad (16)$$

where we have also assumed  $r_{\text{osc}} \ll r_{\text{decay}} \ll 1$ . Using the results (24) and (25) below, the derivatives of the matter fraction  $r_{\text{osc}} = m^2 \sigma_{\text{osc}}^2 / 2\rho_{\text{osc}}$  read

$$\frac{r'_{\text{osc}}}{r_{\text{osc}}} = \frac{2}{\sigma_*}, \quad \frac{r''_{\text{osc}}}{r_{\text{osc}}} = \frac{2}{\sigma_*^2} \quad (17)$$

giving the simple result [45]

$$f_{\text{NL}} = \frac{5}{3} \frac{1}{r_{\text{decay}}}. \quad (18)$$

### 3. Linearised calculations

#### 3.1. Resonance

Our general result in (12) and (13) depends on the quantities  $a_{\text{ref}}$ ,  $\rho_{\text{ref}}$  and  $r_{\text{ref}}$  and their derivatives. Ideally, we would like to be able to calculate them analytically for general parameter values. We first attempt to carry out this calculation in linear theory of resonance [57], i.e. neglecting the backreaction of particles produced during the resonance. This approximation gives a clear physical picture of the resonance, and also an accurate quantitative description of many aspects of it. However, we find that it is not suitable for calculating the curvature perturbation, and, therefore, this calculation acts, ultimately, as a motivation for the nonlinear approach in section 4.

As we assume the  $\chi$  field is heavy during inflation and has a vanishing vacuum expectation value, and that the universe becomes radiation dominated after the end of inflation, the equation of motion for the curvaton is given by

$$\ddot{\sigma} + \frac{3}{2t} \dot{\sigma} + m^2 \sigma = 0, \quad (19)$$

which can easily be put into the canonical form of a Bessel equation. The general solution of (19) which remains bounded as  $t \rightarrow 0$  is given by

$$\sigma(t) = 2^{1/4} \Gamma(5/4) \sigma_* \frac{J_{1/4}(mt)}{(mt)^{1/4}}, \quad (20)$$

where  $J_{1/4}(x)$  is a Bessel function of the first kind and  $\sigma(0) = \sigma_*$  denotes the initial curvaton value set by the dynamics during inflation. In the model (1) that we consider here, the value of the curvaton field is constrained by

$$\frac{H_*^2}{g^2} < \sigma_*^2 < \frac{H_*^2 M_{\text{Pl}}^2}{m^2}, \quad (21)$$

where the upper bound comes from the subdominance of the curvaton and the lower bound is required to keep the  $\chi$  field massive during inflation and to enable broad parametric resonance [54].

The curvaton remains nearly frozen at the value  $\sigma_*$  until the Hubble parameter decreases to  $H \sim m$  and the field starts oscillate around the minimum of its potential. We assume the curvaton is still subdominant at this time and obeys the solution (20).

After the onset of oscillations,  $mt \gtrsim 1$ , (20) can be approximated by the asymptotic expression

$$\sigma(t) \approx \frac{2^{3/4}\Gamma(5/4)}{\pi^{1/2}} \frac{\sigma_*}{(mt)^{3/4}} \sin\left(mt + \frac{\pi}{8}\right). \quad (22)$$

Following the notation of [57], we choose to normalise the scale factor to unity at  $t_{\text{osc}} = 3\pi/(8m)$

$$a = \left(\frac{t}{t_{\text{osc}}}\right)^{1/2} = \left(\frac{8mt}{3\pi}\right)^{1/2}. \quad (23)$$

Up to corrections  $\mathcal{O}(H/m)$ , the energy density of the oscillating curvaton is given by

$$\rho_\sigma = \frac{1}{2} \frac{m^2 \sigma_{\text{osc}}^2}{a^3} \equiv \frac{\rho_{\sigma, \text{osc}}}{a^3}, \quad (24)$$

where  $\sigma_{\text{osc}}$  is the envelope of the oscillatory solution (22) at  $t_{\text{osc}}$

$$\sigma_{\text{osc}} = \frac{8\Gamma(5/4)}{3^{3/4}\pi^{5/4}} \sigma_* \approx 0.76 \sigma_*. \quad (25)$$

The time  $t_{\text{osc}}$  appears as an unphysical reference point in our analysis but as it formally corresponds to a quarter of the first oscillation cycle it can also be thought of as the beginning of curvaton oscillations, hence the subscript.

The coherent curvaton oscillations induce a time-varying effective mass for the  $\chi$  field which can lead to copious production of  $\chi$  particles as discussed in [54]. The process is analogous to the standard inflationary preheating scenario [56, 57, 71], except that the universe is dominated by radiation instead of non-relativistic matter during the resonance. The resonant curvaton decay is efficient if

$$q = \frac{g^2 \sigma_{\text{osc}}^2}{4m^2} \gg 1, \quad (26)$$

which corresponds to broad resonance bands in momentum space. For curvaton values in the range (21) this condition is always satisfied, as one can immediately see by taking into account the lightness of the curvaton during inflation,  $m \ll H_*$ .

Using the solution (22) and applying the analytic methods developed to analyse particle production during the parametric resonance [57], the comoving number density of  $\chi$  particles at late times ( $t \gg t_{\text{osc}}$ ) can be estimated as

$$n_\chi(t) \approx \frac{k_*^3}{64\pi^2 a^3 \sqrt{\mu m t}} e^{2m\mu t}, \quad (27)$$

where  $k_* = (gm\sigma_{\text{osc}})^{1/2}$  and  $\mu \sim 0.14$  is an effective growth index. Due to the stochastic nature of parametric resonance in expanding space, the actual growth index depends very sensitively on other parameters and varies rapidly between 0 and 0.28 between one cycle of oscillation and another.

As the number density of  $\chi$  particles grows exponentially, the contribution to the effective curvaton mass  $g^2\langle\chi^2\rangle$  eventually comes to dominate over the bare mass  $m^2$ . The time  $t_{\text{br}}$  when the two contributions are equal—after which the backreaction of



the  $\chi$  particles can no longer be neglected—is found by equating the number density  $n_\chi \sim \langle \chi^2 \rangle g \sigma$  with  $m^2 \sigma / g$ . Using the result (27), this yields an equation for  $t_{\text{br}}$

$$t_{\text{br}} \approx \frac{1}{4m\mu} \ln \left( \frac{10^5 \mu m (m t_{\text{br}})^{5/2}}{g^5 \sigma_{\text{osc}}} \right), \quad (28)$$

whose solution is given by the  $-1$  branch of Lambert  $W$ -function

$$t_{\text{br}} \approx -\frac{5}{8m\mu} W_{-1} \left( -10^{-2} g^{8/5} \mu^{3/5} q_{\text{osc}}^{1/5} \right). \quad (29)$$

Here  $q_{\text{osc}}$  denotes the value of the resonance parameter (26) at the beginning of oscillations. The result is consistent with the assumption  $t \gg t_{\text{osc}}$  for all  $\mu$  provided that we place the mild constraint  $g^{8/5} q_{\text{osc}}^{1/5} \lesssim 10$ , which corresponds to  $t_{\text{br}} \gtrsim 10 t_{\text{osc}}$ . In this limit (29) can be approximated to reasonable accuracy by

$$t_{\text{br}} \sim \frac{1}{8m\mu} \ln \left( 10^{10} g^{-8} \mu^{-3} q_{\text{osc}}^{-1} \right) + \mathcal{O} \left( m^{-1} \ln(m t_{\text{br}}) \right). \quad (30)$$

The value of the scale factor at the time of backreaction is found by substituting (29) into (23)

$$a_{\text{br}} \approx \left( -\frac{5}{3\pi\mu} \right)^{1/2} W_{-1}^{1/2} \left( -10^{-2} g^{8/5} \mu^{3/5} q_{\text{osc}}^{1/5} \right). \quad (31)$$

The derivatives of  $\ln a_{\text{br}}$  with respect to  $\sigma_*$ , which are needed for computing the curvature perturbation, are

$$(\ln a_{\text{br}})' \approx -\frac{1}{2} (\ln \mu)' - \frac{1}{3\pi\mu a_{\text{br}}^2 \sigma_*} \left( 1 + \mathcal{O}(a_{\text{br}}^{-2}) \right) \quad (32)$$

$$(\ln a_{\text{br}})'' \approx -\frac{1}{2} (\ln \mu)'' + \frac{1}{3\pi\mu a_{\text{br}}^2 \sigma_*^2} \left( 1 + \mathcal{O}(a_{\text{br}}^{-2}) \right), \quad (33)$$

where  $' \equiv \partial / \partial \sigma_*$  and the relation  $\partial^n / \partial \sigma_*^n = (\sigma_{\text{osc}} / \sigma_*)^n \partial^n / \partial \sigma_{\text{osc}}^n$  following from (25) has been used. The terms involving derivatives of the effective growth index  $\mu$  would be very difficult to estimate analytically and we therefore leave them in an implicit form.

Approximate energy conservation  $\frac{1}{2} m^2 \sigma_{\text{br}}^2 + m^2 \sigma_{\text{br}}^2 = 1/2 m^2 \sigma_{\text{osc}}^2 a_{\text{br}}^{-3}$  gives an estimate

$$q_{\text{br}} \approx \frac{1}{12} \frac{g^2 \sigma_{\text{osc}}^2}{m^2 a_{\text{br}}^3} = \frac{1}{3} \frac{q_{\text{osc}}}{a_{\text{br}}^3} \quad (34)$$

for the resonance parameter (26) at the onset of backreaction. If  $q_{\text{br}} \gtrsim 1$ , the resonance does not terminate immediately at  $t_{\text{br}}$ . Instead, the effective curvaton mass  $m_{\text{eff}}^2 = g^2 \langle \chi^2 \rangle$  starts to grow exponentially, which soon brings the resonance to end. The nonlinear stage of the resonance after  $t_{\text{br}}$  therefore makes only a small contribution to the total duration of the resonance [57] which can be reasonably well estimated by the duration of the linear stage  $t_{\text{br}}$  given by (29).

### 3.2. Curvature perturbation

It is not possible to describe the backreaction and the equilibration of the fields using linear theory. To carry out the linearised calculation, we therefore simply assume that the resonance ends instantaneously at time  $t_{\text{br}}$ , and that some fraction  $\xi$  of the curvaton energy is transferred into radiation. The matter and radiation energy densities immediately after backreaction are therefore given by

$$\rho_{m,\text{br}} = (1 - \xi) \frac{\rho_{\sigma,\text{osc}}}{a_{\text{br}}^3}, \quad (35)$$

$$\rho_{r,\text{br}} = \frac{\rho_{r,\text{osc}}}{a_{\text{br}}^4} + \xi \frac{\rho_{\sigma,\text{osc}}}{a_{\text{br}}^3}. \quad (36)$$

In order to calculate the curvature perturbation, we choose this backreaction time as our reference time in (9). Therefore we have  $a_{\text{ref}} = a_{\text{br}}$ , and

$$\rho_{\text{ref}} = \rho_{\text{br}} = \rho_{m,\text{br}} + \rho_{r,\text{br}} = \frac{\rho_{r,\text{osc}}}{a_{\text{br}}^4} + \frac{\rho_{\sigma,\text{osc}}}{a_{\text{br}}^3} \approx \frac{\rho_{\text{osc}}}{a_{\text{br}}^4} (1 + r_{\text{osc}}(a_{\text{br}} - 1)), \quad (37)$$

$$r_{\text{ref}} = r_{\text{br}} = \frac{\rho_{m,\text{br}}}{\rho_{m,\text{br}} + \rho_{r,\text{br}}} = \frac{(1 - \xi)\rho_{\sigma,\text{osc}}a_{\text{br}}}{\rho_{r,\text{osc}} + \rho_{\sigma,\text{osc}}a_{\text{br}}} \approx (1 - \xi)r_{\text{osc}}a_{\text{br}}, \quad (38)$$

where  $r_{\text{osc}} = \rho_{\sigma,\text{osc}}/\rho_{\text{osc}} \approx \rho_{\sigma,\text{osc}}/\rho_{r,\text{osc}}$  and we have assumed that  $r_{\text{osc}}a_{\text{br}} \ll 1$ , which is equivalent to having  $r \ll 1$  throughout the resonance. Substituting these into (12) and (13), we can work out the expression for the curvature perturbation. Using the leading terms in (32), (33), we find

$$(\ln a)' \Big|_{\rho} = \frac{r}{4} \left[ \frac{\xi}{1 - \xi} \frac{a_{\text{br}}}{a} \left( \frac{2}{\sigma_*} - \frac{1}{2} \frac{\mu'}{\mu} + \frac{\xi'}{\xi} \right) + \frac{2}{\sigma_*} - \frac{\xi'}{1 - \xi} \right], \quad (39)$$

$$\begin{aligned} (\ln a)'' \Big|_{\rho} = \frac{r}{4} \left[ \frac{\xi}{1 - \xi} \frac{a_{\text{br}}}{a} \left( \frac{2}{\sigma_*^2} + \frac{4}{\sigma_*} \left( \frac{\xi'}{\xi} - \frac{1}{2} \frac{\mu'}{\mu} \right) + \frac{\xi''}{\xi} + \frac{(\mu^{-1/2})''}{\mu^{-1/2}} - \frac{\xi' \mu'}{\xi \mu} \right) \right. \\ \left. + \frac{2}{\sigma_*^2} - \frac{4\xi'}{\sigma_*(1 - \xi)} - \frac{\xi''}{1 - \xi} \right]. \end{aligned} \quad (40)$$

By setting  $\xi = 0$  in the above expressions, the standard curvaton results (18) for a perturbative decay are recovered.

The terms scaling as  $a^{-1}$  in (39) and (40) represent the contribution due to radiation inhomogeneities created by the curvaton decay. If the curvaton particles left over after the resonance have a long perturbative lifetime, this component effectively redshifts away and the expressions (39) and (40) reduce to

$$(\ln a)' \Big|_{\rho} \sim \frac{r}{2\sigma_*} \left( 1 - \frac{\sigma_* \xi'}{2(1 - \xi)} \right) \quad (41)$$

$$(\ln a)'' \Big|_{\rho} \sim \frac{r}{2\sigma_*^2} \left( 1 - \frac{2\sigma_* \xi'}{1 - \xi} - \frac{\sigma_*^2 \xi''}{2(1 - \xi)} \right). \quad (42)$$

The nonlinearity parameter  $f_{\text{NL}}$  can be computed using (8). In the late time limit, we find using (41) and (42),

$$f_{\text{NL}} \sim \frac{5}{3r} \left( 1 - \frac{2\sigma_* \xi'}{1 - \xi} - \frac{\sigma_*^2 \xi''}{2(1 - \xi)} \right) \left( 1 - \frac{\sigma_* \xi'}{2(1 - \xi)} \right)^{-2}. \quad (43)$$

To make use of these results, one would have to know the first and second derivatives of  $\mu$  and  $\xi$ , which, unfortunately, are difficult to calculate. In principle, the exponential growth rate  $\mu$  is calculable in linearised theory, but obtaining its derivatives reliably is hard because it is an averaged quantity that describes a stochastic process. In contrast,  $\xi$  is fully determined by the nonlinear dynamics at the end of the resonance, and, therefore, it is not possible to calculate it using linearised equations.

We conclude that the perturbations generated by resonant curvaton decay are not calculable using linear theory. Instead, we have to carry out a fully nonlinear calculation using lattice field theory methods.

## 4. Simulations

### 4.1. Simulation method

In section 3 we saw that the curvature perturbations produced by the resonance cannot be calculated using linear theory. Therefore, we adopt a completely different approach. We use nonlinear three-dimensional classical lattice field theory simulations<sup>§</sup> to determine how the scale factor evolves as the fields fall out of equilibrium at the end of preheating and to compute the required quantities  $a_{\text{ref}}$ ,  $\rho_{\text{ref}}$  and  $r_{\text{ref}}$  directly. This is a standard method of solving the field dynamics in such systems [65, 66, 72–77], and recently [37–39] it was shown how it can be used, with the separate universe approximation, to compute curvature perturbations.

The  $\sigma$  and  $\chi$  fields are taken to be position-dependent, and the scale factor  $a$  is homogeneous over the whole lattice. The latter assumption is justified when the lattice is smaller than the Hubble volume, and allows us to describe the expansion of the universe using the Friedmann equation. We have a coupled system of field equations,

$$\ddot{\sigma} + 3H\dot{\sigma} - \frac{1}{a^2}\nabla^2\sigma + m^2\sigma + g^2\sigma\chi^2 = 0 , \quad (44)$$

$$\ddot{\chi} + 3H\dot{\chi} - \frac{1}{a^2}\nabla^2\chi + g^2\sigma^2\chi = 0 . \quad (45)$$

and the Friedmann equation

$$H^2 = \frac{\bar{\rho}}{3M_{\text{Pl}}^2} , \quad (46)$$

where the energy density is calculated as the average energy density in the simulation box,

$$\bar{\rho} = \frac{\rho_{\phi 0}}{a^4} + \frac{1}{L^3} \int d^3x \left[ \frac{1}{2}\dot{\sigma}^2 + \frac{1}{2}\dot{\chi}^2 + \frac{1}{2a^2} ((\nabla\sigma)^2 + (\nabla\chi)^2) + V(\sigma, \chi) \right] . \quad (47)$$

The coupled system of equations (44), (45) and (46) are solved on a comoving lattice with periodic boundary conditions. The inflaton component is included as idealised radiation where  $\rho_{\phi 0}$  is the density in the  $\phi$  field at the beginning of the simulation. We

<sup>§</sup> We use a modification of the corrected version of the code used in refs. [37] and [38] described in the erratum of [38].

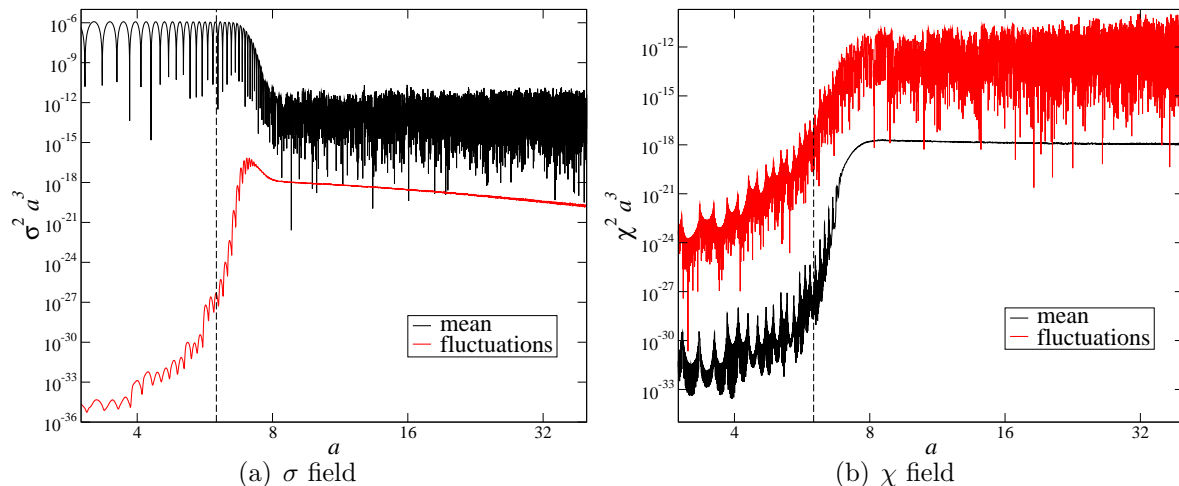


**Figure 1.** Evolution of the fields during one simulation run. To the left of the vertical dashed line the evolution is calculated with (61)-(65); to the right it is calculated with (48)-(52). The  $\phi$  field is included as a homogeneous radiation component.

solve the system in conformal time ( $d\tau = a^{-1}dt$ ) using a fourth order Runge-Kutta algorithm. The system of equations is then

$$\sigma'' + 2\frac{a'}{a}\sigma' - \frac{1}{a^2}\nabla^2\sigma + a^2(m^2\sigma + g^2\sigma\chi^2) = 0, \quad (48)$$

$$\chi'' + 2\frac{a'}{a}\chi' - \frac{1}{a^2}\nabla^2\chi + a^2g^2\sigma^2\chi = 0. \quad (49)$$

The second order Friedmann equation is

$$a'' = \frac{1}{6} \frac{\bar{\rho} - 3\bar{P}}{M_{\text{Pl}}^2} a^3, \quad (50)$$

where the averaged density and pressure are

$$\bar{\rho} = \frac{\rho_{\phi 0}}{a^4} + \frac{1}{L^3} \int d^3x \left[ \frac{1}{2a^2} \left( (\sigma')^2 + (\chi')^2 \right) + \frac{1}{2a^2} \left( (\nabla\sigma)^2 + (\nabla\chi)^2 \right) + V(\sigma, \chi) \right], \quad (51)$$

$$\bar{P} = \frac{\rho_{\phi 0}}{3a^4} + \frac{1}{L^3} \int d^3x \left[ \frac{1}{2a^2} \left( (\sigma')^2 + (\chi')^2 \right) - \frac{1}{6a^2} \left( (\nabla\sigma)^2 + (\nabla\chi)^2 \right) - V(\sigma, \chi) \right]. \quad (52)$$

The initial inflaton energy density  $\rho_{\phi 0}$  depends on the inflaton potential  $V(\phi)$ . For simplicity, we assume it has a quartic form,

$$V(\phi) = \frac{1}{4}\lambda\phi^4. \quad (53)$$

We choose the initial value of  $\phi$  to be  $\phi_0 = M_{\text{Pl}}$ , where we use the subscript 0 to denote the initial values for the simulation. We still have the freedom to choose the value of the conformal time at the start of our simulations. We take

$$\tau_0 = \sqrt{\frac{3}{\lambda}} \frac{M_{\text{Pl}}}{\phi_0^2}, \quad (54)$$

so that the scale factor is simply proportional to conformal time,  $a(\tau) \propto \tau$  even at  $\tau \sim \tau_0$ .

The initial values for the  $\sigma$  and  $\chi$  fields consist of a homogeneous background component  $\sigma_0$  or  $\chi_0$ , which represents fluctuations with wavelength longer than the lattice size, and Gaussian inhomogeneous fluctuations which represent short-distance quantum fluctuations.

The  $\chi$  field is massive during inflation; its long-wavelength fluctuations are heavily suppressed. In contrast, the curvaton field  $\sigma$  is still frozen at the start of the simulation. As a result of superhorizon fluctuations, its local value  $\sigma_*$  at the end of inflation varies between one Hubble patch and another; this sets the initial value  $\sigma_0$  for the curvaton field in our simulation,  $\sigma_0 = \sigma_*$ . By running simulations with different initial curvaton values  $\sigma_0$ , we can, therefore, determine how  $a_{\text{ref}}$ ,  $\rho_{\text{ref}}$  and  $r_{\text{ref}}$  depend on  $\sigma_0$  and calculate the curvature perturbation using (5).

The relevant range of  $\sigma_0$  is determined by the power spectrum  $\mathcal{P}_\sigma(k)$  of the curvaton field. Assuming that the curvaton mass  $m$  is very small, the power spectrum is given by

$$\mathcal{P}_\sigma(k) \approx \frac{H_k^2}{4\pi^2} \approx \frac{4}{3\pi^2} \lambda M_{\text{Pl}}^2 N_k^2 \quad (55)$$

where  $H_k$  and  $N_k$  are the Hubble rate and the number of  $e$ -foldings before the end of inflation evaluated at the time when the mode  $k = aH_k$  left the horizon. A more accurate calculation for non-zero  $m$  is given in appendix 1 of [38].

To completely determine the observable curvature perturbation, we need to run the simulation for all values of  $\sigma_*$  that were realised in our current Hubble volume. The curvaton field is a Gaussian random field, so the mean value over a Hubble volume today,  $\overline{\sigma_*}$ , has a Gaussian distribution. The variance of this distribution is

$$\langle \overline{\sigma_*^2} \rangle = \int_{N_0}^{N_{\text{tot}}} \mathcal{P}_\sigma(k) \left(1 - \frac{1}{N_k}\right) dN_k \approx \frac{4}{9\pi^2} \lambda M_{\text{Pl}}^2 N_{\text{tot}}^3 . \quad (56)$$

Note that this depends on  $N_{\text{tot}}$ , the total number of  $e$ -foldings of inflation, so is essentially a free variable. This distribution is centred around zero, assuming no homogeneous classical curvaton background.

The width of the range of  $\sigma_*$  that we need to cover is given by the variance of  $\sigma_*$  within our current Hubble volume, between different Hubble volumes at the end of inflation. This is given by

$$\langle \delta\sigma_*^2 \rangle = \int_0^{N_0} \mathcal{P}_\sigma(k) \left(1 - \frac{1}{N_k}\right) dN_k \approx \frac{4}{9\pi^2} \lambda M_{\text{Pl}}^2 N_0^3 , \quad (57)$$

where  $N_0 \approx 60$  is the number of  $e$ -foldings after the largest currently observable scales left the horizon. This gives the width of the range of  $\sigma_*$  that we need to consider. Note that the only free parameter this depends on is  $\lambda$ .

For the initial values of the inhomogeneous field modes, we follow the standard approach [65,66,72,73,75]. The  $\chi$  field is given random initial conditions from a Gaussian distribution whose two-point functions are the same as those in the tree-level quantum vacuum state,

$$\langle \chi_{\mathbf{k}}^* \chi_{\mathbf{q}} \rangle = (2\pi)^3 \delta(\mathbf{k} - \mathbf{q}) \frac{1}{2\omega_{\mathbf{k}}} ,$$

$$\langle \dot{\chi}_{\mathbf{k}}^* \dot{\chi}_{\mathbf{q}} \rangle = (2\pi)^3 \delta(\mathbf{k} - \mathbf{q}) \frac{\omega_{\mathbf{k}}}{2}, \quad (58)$$

where  $\omega_{\mathbf{k}} = \sqrt{k^2 + m_\chi^2} = \sqrt{k^2 + g^2 \sigma_0^2}$ . All other two-point correlators vanish. The inhomogeneous modes of  $\sigma$  are populated similarly to those of  $\chi$ .

In order to estimate the error bars in, for example, figure 3 we repeat each simulation with the same parameters multiple times using different realisations of the above random initial conditions. In earlier work on preheating [37–39], the whole evolution was calculated using full nonlinear equations. In the current case that would be computationally very expensive, because the model is not conformally invariant and the universe expands by a large factor  $\sim 100$  during the evolution. To fit the relevant wavelengths inside the lattice throughout the whole simulation, the lattice size would have to be much larger than  $100^3$ , which is not possible given the number of simulations which need to be run.

Instead, we take a shortcut, and make use of the fact that until the magnitude of the fluctuations in  $\chi$  become large enough to backreact on  $\sigma$  (when  $\langle \chi^2 \rangle \sim m^2/g^2$ ) the field dynamics are linear to a very good approximation. Therefore, we can evolve the whole probability distributions of the initial conditions in  $k$ -space using linearised versions of (48)-(52). More precisely, we need to solve the linear equations for the inhomogeneous modes,

$$\sigma_{\mathbf{k}}'' + 2\frac{a'}{a}\sigma_{\mathbf{k}}' + k^2\sigma_{\mathbf{k}} + a^2 m^2 \sigma_{\mathbf{k}} = 0, \quad (59)$$

$$\chi_{\mathbf{k}}'' + 2\frac{a'}{a}\chi_{\mathbf{k}}' + k^2\chi_{\mathbf{k}} + a^2 g^2 \sigma^2 \chi_{\mathbf{k}} = 0, \quad (60)$$

in the background provided by the solutions of the nonlinear equations for the homogeneous modes,

$$\sigma'' + 2\frac{a'}{a}\sigma' + a^2 (m^2\sigma + g^2\sigma\chi^2) = 0, \quad (61)$$

$$\chi'' + 2\frac{a'}{a}\chi' + a^2 g^2 \sigma^2 \chi = 0, \quad (62)$$

$$a'' = \frac{1}{6} \frac{\rho - 3P}{M_{\text{Pl}}^2} a^3, \quad (63)$$

$$\rho = \frac{\rho_{\phi 0}}{a^4} + \frac{1}{2a^2} \left( (\sigma')^2 + (\chi')^2 \right) + V(\sigma, \chi), \quad (64)$$

$$P = \frac{\rho_{\phi 0}}{3a^4} + \frac{1}{2a^2} \left( (\sigma')^2 + (\chi')^2 \right) - V(\sigma, \chi). \quad (65)$$

The background solution is independent of the modes in (59) and (60), and therefore it needs to be calculated only once for each  $\sigma_0$ .

Crucially, the general solution of the linear mode (59) and (60) is obtained by solving the equations for two different initial values. This is because, as a consequence of linearity, the general solution can be represented as

$$\begin{pmatrix} \chi_{\mathbf{k}}(\tau) \\ \chi'_{\mathbf{k}}(\tau) \end{pmatrix} = M(\tau) \begin{pmatrix} \chi_{\mathbf{k}}(0) \\ \chi'_{\mathbf{k}}(0) \end{pmatrix}, \quad (66)$$

where  $M(\tau)$  is a two-by-two matrix. Consider now the solutions with initial conditions of position 1 and velocity 0 and vice versa:

$$\begin{pmatrix} \chi_{\mathbf{k}(1,0)}(\tau) \\ \chi'_{\mathbf{k}(1,0)}(\tau) \end{pmatrix} = M(\tau) \begin{pmatrix} 1 \\ 0 \end{pmatrix}, \quad (67)$$

$$\begin{pmatrix} \chi_{\mathbf{k}(0,1)}(\tau) \\ \chi'_{\mathbf{k}(0,1)}(\tau) \end{pmatrix} = M(\tau) \begin{pmatrix} 0 \\ 1 \end{pmatrix}. \quad (68)$$

Linearity implies that the solution of arbitrary initial conditions  $\chi_{\mathbf{k}}(0)$  and  $\chi'_{\mathbf{k}}(0)$  is given simply by

$$\begin{pmatrix} \chi_{\mathbf{k}}(\tau) \\ \chi'_{\mathbf{k}}(\tau) \end{pmatrix} = \chi_{\mathbf{k}}(0) \begin{pmatrix} \chi_{\mathbf{k}(1,0)}(\tau) \\ \chi'_{\mathbf{k}(1,0)}(\tau) \end{pmatrix} + \chi'_{\mathbf{k}}(0) \begin{pmatrix} \chi_{\mathbf{k}(0,1)}(\tau) \\ \chi'_{\mathbf{k}(0,1)}(\tau) \end{pmatrix}. \quad (69)$$

We use this approach to evolve the fields until some scale factor  $a_1$ , which is well before the nonlinear terms become important. Only then, we Fourier transform the fields to coordinate space and start to evolve them using the full nonlinear equations (48)-(52). This is shown in figure 1. We checked that our results do not depend on the chosen value of  $a_1$ .

This method has two advantages which make the calculation presented here possible. Firstly, we evolve the whole distribution, so the linear evolution only needs to be calculated once, and only the relatively short nonlinear stage has to be repeated for each realisation of the initial conditions. Secondly, and more significantly, it reduces the factor by which the universe grows during the evolution of (48)-(52) from  $\sim 100$  to  $\sim 10$ . This allow us to use lattices with much lower resolution to achieve comparably accurate results, thus significantly reducing computation time.

#### 4.2. Simulation results

Our model has three free parameters,  $\lambda$ ,  $m$ ,  $g$ . It is not possible for us to probe this whole parameter space using current computational technology. Therefore, we simply pick one set of parameters,  $\lambda = 10^{-16}$ ,  $g = 0.01$  and  $m = 10^{-8}M_{\text{Pl}}$ . We take  $\chi_0 = 10^{-16}M_{\text{Pl}}$ .

We also have to choose the initial value of the curvaton field  $\sigma$ . In order to cover all values of  $\sigma_*$  in our currently observable universe, we carried out simulations for a range of  $\sigma_0$

$$\overline{\sigma}_0 - \frac{1}{2}\delta\sigma_0 \leq \sigma_0 \leq \overline{\sigma}_0 + \frac{1}{2}\delta\sigma_0, \quad (70)$$

whose width is given by (57),

$$\delta\sigma_0 \approx \sqrt{\langle \delta\sigma_*^2 \rangle} \approx 10^{-6}M_{\text{Pl}}. \quad (71)$$

The probability distribution of the central value  $\overline{\sigma}_0$  is given by (56), but as a results of its dependence on the total number of e-foldings  $N_{\text{tot}}$ , which is unknown, we can essentially choose it freely. Nevertheless, the value of  $\overline{\sigma}_0$  is restricted by several constraints. The resonance being brought to an end by backreaction demands that  $q \gg 1$  (see (26)). The characteristic frequency of the  $\chi$  field oscillations is  $g\sigma_0$  and the time the system

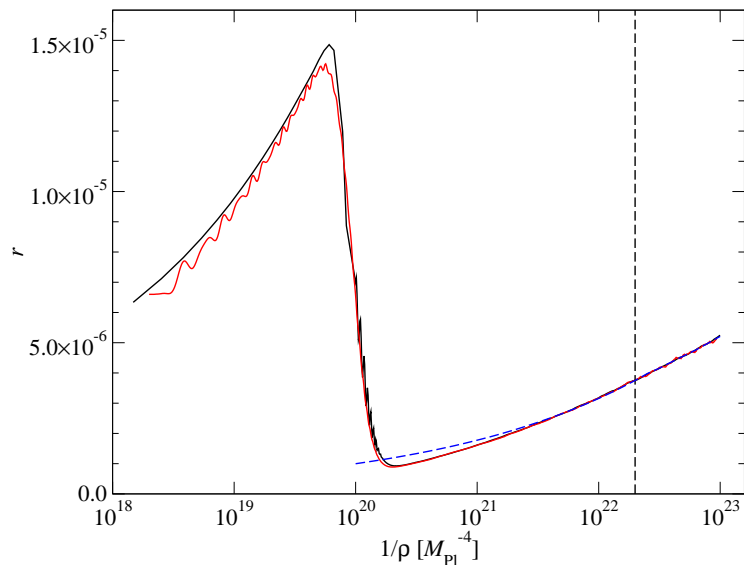


**Figure 2.** The matter fraction  $r$  during one simulation. The resonance is rapid and destroys  $\sim 95\%$  of the matter. The two solid lines show the two definitions of  $r$  given in (73) and (74).  $\rho_{\text{ref}} = 5 \times 10^{-23}$  is marked by the vertical dashed line. The blue dashed line represents the approximation (9) taken about this  $\rho_{\text{ref}}$

takes to reach backreaction is proportional to  $m^{-1}$ . Therefore, the simulation time is proportional to  $g\sigma_0/m = 2q^{1/2}$ . In our simulations we used three values:

$$\bar{\sigma}_0 = 0.0005M_{\text{Pl}}, \quad 0.001M_{\text{Pl}} \quad \text{and} \quad 0.002M_{\text{Pl}}. \quad (72)$$

These corresponds to  $q_{br} \approx 50, 200$  and  $750$  respectively. With these parameters one  $32^3$  point lattice simulation takes  $\sim 3$  hours. We repeat each simulation several ( $\sim 50$ ) times with different random realisations of initial conditions to obtain statistical errors. Although, this computational method is very resource intensive, the independence of each simulation (or Hubble patch) means that the problem scales perfectly on a multiprocessor machine. A time-step of  $(2 \times 10^{-4}/m)M_{\text{Pl}}^{-1}$  and lattice spacing of  $(5m/96)M_{\text{Pl}}^{-1}$  were used.

Each simulation gives us time-streams of the scale factor  $a$ , the density  $\rho$ , given by (51), and the pressure  $P$ , given by (52). We measure the matter fraction  $r = \rho_m/\rho$  in two different ways: from the ratio of the pressure and energy density,

$$r = 1 - 3\frac{P}{\rho}, \quad (73)$$

and by fitting the dependence of the scale factor on the energy density,

$$\log a = -\frac{1}{4-r} \log \rho + \text{constant}, \quad (74)$$

in a narrow range about the point of interest. In continuous time these two expressions would agree, and therefore any discrepancy between them would be a sign of time discretisation errors.



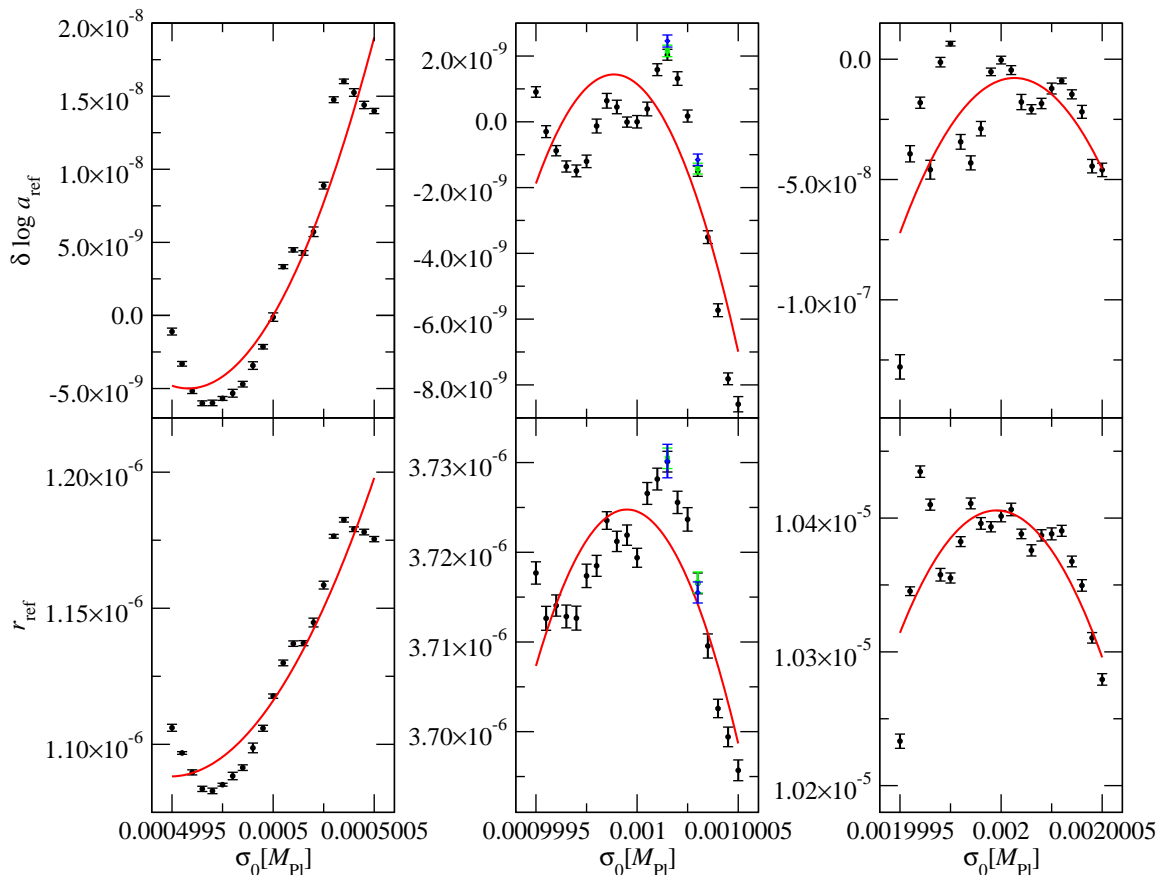


**Figure 3.** Results from simulations for different ranges of  $\sigma_0$  centred around  $\bar{\sigma}_0 = 0.0005M_{\text{Pl}}$ ,  $\bar{\sigma}_0 = 0.001M_{\text{Pl}}$  and  $\bar{\sigma}_0 = 0.002M_{\text{Pl}}$ , each covering the values present in one Hubble volume today. The top and bottom rows show  $\ln a_{\text{ref}}$  and  $r_{\text{ref}}$  respectively measured at  $\rho = 5 \times 10^{-23}M_{\text{Pl}}^4$  and averaged over 10 – 50 runs. The solid lines show quadratic fits of the form (75). The centre panels also show some numerical checks of the simulation results. The green (square) points represent simulations with time-steps double the length of the black points. The blue (diamond) points are represent a four times longer time-step. It can be seen that the results are within the errors of the primary runs.

The measured matter fraction  $r$  is shown in figure 2 as a function of the energy density. The two curves correspond to the two definitions (73) and (74), which clearly agree very well. Initially, it grows because the matter component decreases more slowly than the radiation component. At  $\rho^{-1} \approx 10^{20}M_{\text{Pl}}^{-4}$ , it drops rapidly as the resonance destroys most of the curvatons. Afterwards  $r$  again grows as the universe expands.

To calculate the curvature perturbation using (12) and (13), we need to choose a reference point at which we measure the scale factor  $a_{\text{ref}}$ , energy density  $\rho_{\text{ref}}$  and matter fraction  $r_{\text{ref}}$ . We chose this be at fixed energy density  $\rho_{\text{ref}} = 5 \times 10^{-23}M_{\text{Pl}}^4$ . We interpolated our measurements using a simple least-squares fit in  $\{\log(\rho), \log(a)\}$  and  $\{\log(\rho), \log(r)\}$  about  $\rho = \rho_{\text{ref}}$  to find the scale factor  $a_{\text{ref}}$  and the matter fraction  $r_{\text{ref}}$ . The results are shown in figure 3 for three choices of  $\bar{\sigma}_0$ .

We found that the choice of  $\rho_{\text{ref}}$  has no effect on the results as long as it is well after the end of the resonance. This is demonstrated by figure 2, in which the (blue) dashed curve shows the matter fraction  $r$  calculated from the assumption (9) of non-interacting matter and radiation components with the measured values of  $a_{\text{ref}}$  and  $r_{\text{ref}}$ . This agrees very well with the measured  $r(\rho)$  at late times.

We calculate the first and second derivatives of  $\ln a_{\text{ref}}$  and  $r_{\text{ref}}$  with respect to  $\sigma_0$ . Assuming that the expansion (5) works well over the whole range of  $\sigma_0$  in the current Hubble volume, we do this by fitting quadratic polynomials

$$\begin{aligned}\ln a_{\text{ref}}(\sigma_0) &= \ln a_{\text{ref}}(\bar{\sigma}_0) + \ln a'_{\text{ref}}(\sigma_0 - \bar{\sigma}_0) + \frac{1}{2} \ln a''_{\text{ref}}(\sigma_0 - \bar{\sigma}_0)^2, \\ r_{\text{ref}}(\sigma_0) &= r_{\text{ref}}(\bar{\sigma}_0) + r'_{\text{ref}}(\sigma_0 - \bar{\sigma}_0) + \frac{1}{2} r''_{\text{ref}}(\sigma_0 - \bar{\sigma}_0)^2,\end{aligned}\quad (75)$$

to our data. These fits are shown by the curves in figure 3 and the corresponding fit parameters are given in table 1.

We concentrate on two measurable quantities: the spectrum of curvature perturbations  $\mathcal{P}_\zeta$ , which is given by (6), and the nonlinearity parameter  $f_{\text{NL}}$ , which is given by (8). We chose to fix  $\rho_{\text{ref}}$  to be a constant, so (12) and (13) simplify to

$$(\ln a)' \Big|_\rho = (\ln a_{\text{ref}})' + \frac{r_{\text{decay}} - r_{\text{ref}}}{4} \frac{r'_{\text{ref}}}{r_{\text{ref}}}, \quad (76)$$

$$(\ln a)'' \Big|_\rho = (\ln a_{\text{ref}})'' + \frac{r_{\text{decay}} - r_{\text{ref}}}{4} \frac{r''_{\text{ref}}}{r_{\text{ref}}}. \quad (77)$$

For the amplitude of the curvature perturbations to agree with observations,  $\mathcal{P}_\zeta \approx 10^{-10}$ , (6) and (76) imply

$$r_{\text{decay}} = r_{\text{ref}} + 4 \frac{r_{\text{ref}}}{r'_{\text{ref}}} \left[ \pm \sqrt{\frac{\mathcal{P}_\zeta}{\mathcal{P}_\sigma}} - (\ln a_{\text{ref}})' \right]. \quad (78)$$

Using this, the nonlinearity parameter (8) can be recast in the form

$$f_{\text{NL}} = \frac{5}{6} \frac{\mathcal{P}_\sigma}{\mathcal{P}_\zeta} \left( (\ln a_{\text{ref}})'' + \frac{r''_{\text{ref}}}{r'_{\text{ref}}} \left( \pm \sqrt{\frac{\mathcal{P}_\zeta}{\mathcal{P}_\sigma}} - (\ln a_{\text{ref}})' \right) \right). \quad (79)$$

The spectrum of the curvaton fluctuations produced during inflation is given by (55), which, for our parameters is,  $\mathcal{P}_\sigma \approx 5 \times 10^{-14} M_{\text{Pl}}^2$ , so that  $\sqrt{\mathcal{P}_\zeta/\mathcal{P}_\sigma} \approx 45$ .

The values of  $r_{\text{decay}}$  and  $f_{\text{NL}}$  calculated from the fit parameters are shown in table 2. In all cases  $r_{\text{decay}}$  has an acceptable value,  $r_{\text{ref}} \ll r_{\text{decay}} \ll 1$ , which means that the curvaton can produce perturbations with the observed amplitude. On the other hand,  $f_{\text{NL}}$  is much larger than the observations allow [1–3, 70], which rules out these parameter values.

Note that these values of  $r_{\text{decay}}$  and  $f_{\text{NL}}$  rely on the quadratic fit (75), which clearly does not describe the data very well, as can be seen in figure 3. This illustrates that the curvature perturbations produced in this model are not well approximated by truncating the expansion (7) at second order and parameterising the non-Gaussian effects only by local  $f_{\text{NL}}$ . Therefore one should not put too much emphasis on the precise numbers, but

$\bar{\sigma}_0$	0.0005	0.001	0.002
$(\ln a_{\text{ref}})'$	$0.024 \pm 0.002$	$-0.005 \pm 0.001$	$0.025 \pm 0.016$
$(\ln a_{\text{ref}})''$	$57000 \pm 13000$	$-44000 \pm 9000$	$-420000 \pm 120000$
$r_{\text{ref}}$	$(1.116 \pm 0.004) \times 10^{-6}$	$(3.72 \pm 0.002) \times 10^{-6}$	$(10.4 \pm 0.011) \times 10^{-6}$
$r'_{\text{ref}}$	$0.109 \pm 0.008$	$-0.009 \pm 0.004$	$-0.014 \pm 0.024$
$r''_{\text{ref}}$	$(2.1 \pm 0.6) \times 10^5$	$(1.7 \pm 0.3) \times 10^5$	$(-8.3 \pm 1.8) \times 10^5$

**Table 1.** Fit parameters defined in (75) in Planck units.

$\bar{\sigma}_0$	0.0005	0.001	0.002
$r_{\text{decay}}$	$0.0018 \pm 0.0001$	$0.08 \pm 0.03$	$0.13 \pm 0.21$
$f_{\text{NL}}$	$(3.6 \pm 1.0) \times 10^4$	$(-3.7 \pm 1.7) \times 10^5$	$(-1.0 \pm 1.8) \times 10^6$
$r_{\text{decay}}^{\text{pert}}$	0.046	0.091	0.182
$f_{\text{NL}}^{\text{pert}}$	36	18	9

**Table 2.** The values of  $r_{\text{decay}}$  and  $f_{\text{NL}}$  calculated using (78) and (79) with the full simulation data (upper) and in the standard perturbative curvaton theory (lower).

the conclusion that the predicted perturbations are highly non-Gaussian and ruled out by current observations.

However, our calculations are non-perturbative and we are not limited to the usual Taylor expansion in (5). Instead, using (10) we obtain the whole function  $\zeta(\sigma_*)$  as a simple linear combination

$$\zeta(\sigma_*) = \ln a(\sigma_*) - \ln a(\bar{\sigma}_*) = \delta \ln a_{\text{ref}}(\sigma_*) + C \delta r_{\text{ref}}(\sigma_*), \quad (80)$$

where the constant  $C$  depends on the perturbative curvaton decay rate  $\Gamma$  and is given by

$$C = \frac{1}{4} \left[ \left( \frac{\rho_{\text{ref}}}{\rho_{\text{decay}}} \right)^{1/4} - 1 \right] = \frac{1}{4} \left( \frac{r_{\text{decay}}}{r_{\text{ref}}} - 1 \right). \quad (81)$$

In figure 4 we show this full result for the three choices of  $\bar{\sigma}_0$ , calculated with the values of  $r_{\text{decay}}$  shown in Table 2. These results give a complete description of the statistics of curvature perturbations in this model, and they could be used to produce maps of the CMB or to compare directly with observations. The correct way to calculate  $f_{\text{NL}}$  and other nonlinearity parameters describing higher order statistics from our results would, therefore, be to repeat the precise procedure the observers use in their measurements. The data are not well approximated by (7) truncated at second order, so different ways of doing this would probably yield very different values for  $f_{\text{NL}}$ . Also,  $f_{\text{NL}}$  and other nonlinearity parameters would also probably appear to be scale and position dependent, because on smaller scales one would cover a smaller range of  $\sigma_*$ .

Figure 3 shows that, with our parameters,  $\delta \ln a_{\text{ref}}$  is orders of magnitude smaller than the amplitude of the observed perturbations, and, therefore, the dominant

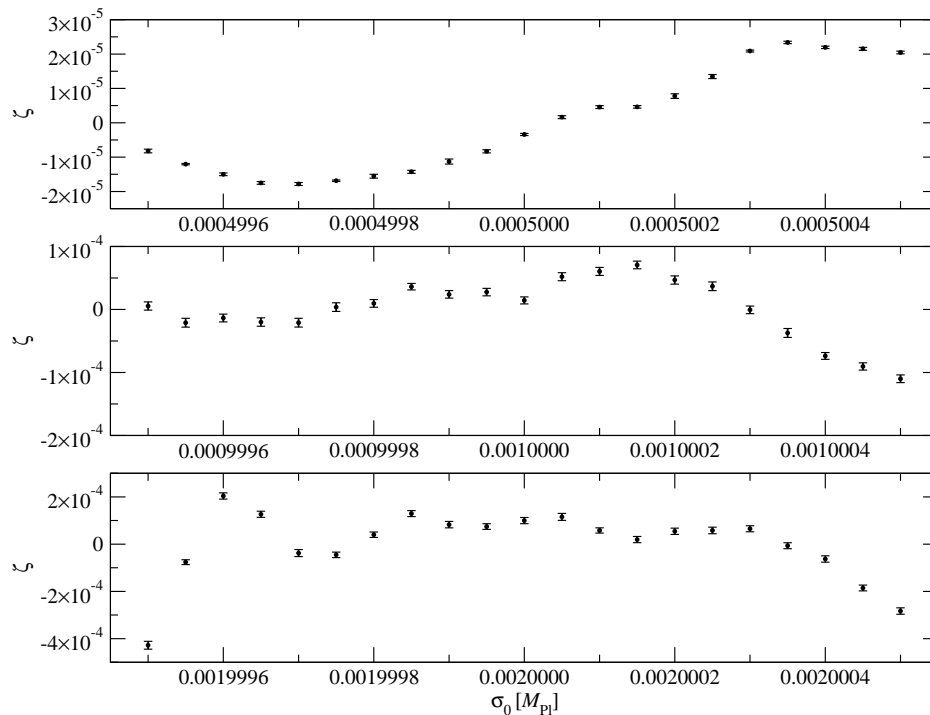


**Figure 4.** The curvature perturbation (4) as a function of the curvaton field value for the three cases (from top to bottom)  $\bar{\sigma}_0 = 0.0005 M_{\text{Pl}}$ ,  $0.001 M_{\text{Pl}}$ ,  $0.002 M_{\text{Pl}}$ , calculated using (80) with the value of  $r_{\text{decay}}$  taken from table 2. In each case, the dependence is highly nonlinear, implying strong non-Gaussianity.

contribution to (80) must come from the second term, i.e. from the variation of the matter fraction  $r_{\text{ref}}$ . Figure 2 shows that the matter fraction drops by a factor of around 20 during the nonlinear stage, but in itself, this drop has no effect on the properties of the final perturbations, because it could be fully compensated for by reducing  $\rho_{\text{decay}}$ . Instead, what is important is that the amount of curvatons left after the nonlinear stage depends sensitively on the value of  $\sigma_*$ . This leads to the variation of  $r_{\text{ref}}$  within the range of  $\sigma_*$  present in one Hubble volume, which is seen in figure 3 and which makes the dominant contribution to the curvature perturbations.

We believe that the sensitive dependence on  $\sigma_*$  is caused by the nonlinear field dynamics at the end of the resonance, but we do not have a detailed explanation of this. Nevertheless, it is in qualitative agreement with the results found in [57, 76] for inflationary preheating, and with findings that the resonance dynamics in massless preheating are effectively chaotic and that small variations in initial conditions can have a great impact on curvature perturbations [39]. In the current case the dependence seems smooth, suggesting that the dynamics are not strictly chaotic.

## 5. Conclusions

In this work we have presented a method of calculating the curvature perturbations from resonant curvaton decay. The curvaton field is light relative to the Hubble rate during inflation and, as a result, its fluctuations are correlated on superhorizon scales; the mean value of the curvaton field varies between one Hubble volume and another. The local value of the curvaton field affects both the amount of expansion and the fraction of the curvaton particles which are destroyed during resonant decay into another field. This turns fluctuations of the curvaton field into curvature perturbations, which are generally non-Gaussian. As the field evolution at the end of the resonance is nonlinear, these perturbations cannot be calculated using standard perturbative techniques.

We computed this effect numerically using classical field theory simulations combined with the  $\delta N$  approach. This approach was used earlier in refs. [37–39], but the current case is technically more difficult because the model is not scale invariant. To deal with this, we divided the evolution into three parts: First, the inhomogeneous modes were evolved numerically using linearised equations. Shortly before nonlinearities become important, we switched to a full nonlinear simulation to describe the non-equilibrium dynamics at the end of the resonance. Eventually, when the system has equilibrated, we extrapolated to late times by assuming that the universe consists of non-interacting matter and radiation. This approach allowed us to study evolution during which the universe expands by several orders of magnitude, which would not be possible using a straightforward field theory simulation.

Our method is fully nonperturbative; we are not forced to assume that the non-Gaussianity is of the simple form (7) parameterised by  $f_{\text{NL}}$ , and indeed we find that, at least at our parameter values, it is not. This may well be a fairly generic consequence of nonlinear field evolution. Instead, our method produces the full numerical dependence of the curvature perturbation  $\zeta$  on the curvaton field  $\sigma_*$ , which is a Gaussian random variable with a known power spectrum. More work is needed to properly compare such data with observations.

Our findings demonstrate that the curvaton resonance can leave a significant imprint on primordial perturbations. At the parameter values we studied the perturbations were far too non-Gaussian to be compatible with observations, but it is very likely that there are other parameter values with acceptable levels of non-Gaussianity. Therefore it would be interesting to explore a wider range of parameters in future work. In this work we focused on parameters for which the curvaton is subdominant throughout the whole evolution and the decay product field  $\chi$  is massive during inflation, but the other possibilities are equally important and worth investigating in future work. We also expect a very similar resonance to take place in a model in which the curvaton is charged under a gauge group and decays resonantly into gauge bosons.

## Acknowledgements

This work was supported by the Science and Technology Facilities Council and by the Academy of Finland grant 130265 and made use of the Imperial College High Performance Computing Service||. The authors would also like to thank Kari Enqvist for valuable discussions.

## References

- [1] E. Komatsu *et al.*, *Five-Year Wilkinson Microwave Anisotropy Probe Observations: Cosmological Interpretation*, *Astrophys. J. Suppl.* **180** (2009) 330–376, [[arXiv:0803.0547](#)].
- [2] A. P. S. Yadav and B. D. Wandelt, *Evidence of Primordial Non-Gaussianity ( $f_{\text{NL}}$ ) in the Wilkinson Microwave Anisotropy Probe 3-Year Data at  $2.8\sigma$* , *Phys. Rev. Lett.* **100** (2008) 181301, [[arXiv:0712.1148](#)].
- [3] E. Komatsu *et al.*, *Non-Gaussianity as a Probe of the Physics of the Primordial Universe and the Astrophysics of the Low Redshift Universe*, [arXiv:0902.4759](#).
- [4] J. M. Maldacena, *Non-Gaussian features of primordial fluctuations in single field inflationary models*, *JHEP* **05** (2003) 013, [[astro-ph/0210603](#)].
- [5] N. Bartolo, S. Matarrese, and A. Riotto, *Non-Gaussianity from inflation*, *Phys. Rev.* **D65** (2002) 103505, [[hep-ph/0112261](#)].
- [6] V. Acquaviva, N. Bartolo, S. Matarrese, and A. Riotto, *Second-order cosmological perturbations from inflation*, *Nucl. Phys.* **B667** (2003) 119–148, [[astro-ph/0209156](#)].
- [7] D. Seery and J. E. Lidsey, *Primordial non-gaussianities from multiple-field inflation*, *JCAP* **0509** (2005) 011, [[astro-ph/0506056](#)].
- [8] X. Chen, M.-x. Huang, S. Kachru, and G. Shiu, *Observational signatures and non-Gaussianities of general single field inflation*, *JCAP* **0701** (2007) 002, [[hep-th/0605045](#)].
- [9] N. Arkani-Hamed, P. Creminelli, S. Mukohyama, and M. Zaldarriaga, *Ghost Inflation*, *JCAP* **0404** (2004) 001, [[hep-th/0312100](#)].
- [10] M. Alishahiha, E. Silverstein, and D. Tong, *DBI in the sky*, *Phys. Rev.* **D70** (2004) 123505, [[hep-th/0404084](#)].
- [11] D. Seery and J. E. Lidsey, *Primordial non-gaussianities in single field inflation*, *JCAP* **0506** (2005) 003, [[astro-ph/0503692](#)].
- [12] P. Creminelli, *On non-gaussianities in single-field inflation*, *JCAP* **0310** (2003) 003, [[astro-ph/0306122](#)].
- [13] D. Langlois, S. Renaux-Petel, D. A. Steer, and T. Tanaka, *Primordial perturbations and non-Gaussianities in DBI and general multi-field inflation*, *Phys. Rev.* **D78** (2008) 063523, [[arXiv:0806.0336](#)].
- [14] F. Arroja, S. Mizuno, and K. Koyama, *Non-gaussianity from the bispectrum in general multiple field inflation*, *JCAP* **0808** (2008) 015, [[arXiv:0806.0619](#)].
- [15] X. Chen, B. Hu, M.-x. Huang, G. Shiu, and Y. Wang, *Large Primordial Trispectra in General Single Field Inflation*, *JCAP* **0908** (2009) 008, [[arXiv:0905.3494](#)].
- [16] F. Arroja, S. Mizuno, K. Koyama, and T. Tanaka, *On the full trispectrum in single field DBI-inflation*, *Phys. Rev.* **D80** (2009) 043527, [[arXiv:0905.3641](#)].
- [17] X. Chen, R. Easther, and E. A. Lim, *Large non-Gaussianities in single field inflation*, *JCAP* **0706** (2007) 023, [[astro-ph/0611645](#)].
- [18] X. Chen, R. Easther, and E. A. Lim, *Generation and Characterization of Large Non-Gaussianities in Single Field Inflation*, *JCAP* **0804** (2008) 010, [[arXiv:0801.3295](#)].

|| <http://www.imperial.ac.uk/ict/services/teachingandresearchservices/highperformancecomputing>

- [19] F. Bernardeau and J.-P. Uzan, *Non-Gaussianity in multi-field inflation*, *Phys. Rev.* **D66** (2002) 103506, [[hep-ph/0207295](#)].
- [20] F. Bernardeau and J.-P. Uzan, *Inflationary models inducing non-gaussian metric fluctuations*, *Phys. Rev.* **D67** (2003) 121301, [[astro-ph/0209330](#)].
- [21] D. H. Lyth, *Generating the curvature perturbation at the end of inflation*, *JCAP* **0511** (2005) 006, [[astro-ph/0510443](#)].
- [22] M. P. Salem, *On the generation of density perturbations at the end of inflation*, *Phys. Rev.* **D72** (2005) 123516, [[astro-ph/0511146](#)].
- [23] M. Sasaki, *Multi-brid inflation and non-Gaussianity*, *Prog. Theor. Phys.* **120** (2008) 159–174, [[arXiv:0805.0974](#)].
- [24] A. Naruko and M. Sasaki, *Large non-Gaussianity from multi-brid inflation*, *Prog. Theor. Phys.* **121** (2009) 193–210, [[arXiv:0807.0180](#)].
- [25] C. T. Byrnes, K.-Y. Choi, and L. M. H. Hall, *Conditions for large non-Gaussianity in two-field slow-roll inflation*, *JCAP* **0810** (2008) 008, [[arXiv:0807.1101](#)].
- [26] C. T. Byrnes, K.-Y. Choi, and L. M. H. Hall, *Large non-Gaussianity from two-component hybrid inflation*, *JCAP* **0902** (2009) 017, [[arXiv:0812.0807](#)].
- [27] C. T. Byrnes and G. Tasinato, *Non-Gaussianity beyond slow roll in multi-field inflation*, *JCAP* **0908** (2009) 016, [[arXiv:0906.0767](#)].
- [28] L. Kofman, *Probing string theory with modulated cosmological fluctuations*, [astro-ph/0303614](#).
- [29] G. Dvali, A. Gruzinov, and M. Zaldarriaga, *A new mechanism for generating density perturbations from inflation*, *Phys. Rev.* **D69** (2004) 023505, [[astro-ph/0303591](#)].
- [30] K. Ichikawa, T. Suyama, T. Takahashi, and M. Yamaguchi, *Primordial Curvature Fluctuation and Its Non-Gaussianity in Models with Modulated Reheating*, *Phys. Rev.* **D78** (2008) 063545, [[arXiv:0807.3988](#)].
- [31] C. T. Byrnes, *Constraints on generating the primordial curvature perturbation and non-Gaussianity from instant preheating*, *JCAP* **0901** (2009) 011, [[arXiv:0810.3913](#)].
- [32] K. Enqvist, A. Jokinen, A. Mazumdar, T. Multamaki, and A. Vaihkonen, *Non-Gaussianity from Preheating*, *Phys. Rev. Lett.* **94** (2005) 161301, [[astro-ph/0411394](#)].
- [33] K. Enqvist, A. Jokinen, A. Mazumdar, T. Multamaki, and A. Vaihkonen, *Non-gaussianity from instant and tachyonic preheating*, *JCAP* **0503** (2005) 010, [[hep-ph/0501076](#)].
- [34] N. Barnaby and J. M. Cline, *Nongaussian and nonscale-invariant perturbations from tachyonic preheating in hybrid inflation*, *Phys. Rev.* **D73** (2006) 106012, [[astro-ph/0601481](#)].
- [35] N. Barnaby and J. M. Cline, *Nongaussianity from Tachyonic Preheating in Hybrid Inflation*, *Phys. Rev.* **D75** (2007) 086004, [[astro-ph/0611750](#)].
- [36] K. Kohri, D. H. Lyth, and C. A. Valenzuela-Toledo, *On the generation of a non-gaussian curvature perturbation during preheating*, [arXiv:0904.0793](#).
- [37] A. Chambers and A. Rajantie, *Lattice calculation of non-Gaussianity from preheating*, *Phys. Rev. Lett.* **100** (2008) 041302, [[arXiv:0710.4133](#)].
- [38] A. Chambers and A. Rajantie, *Non-Gaussianity from massless preheating*, *JCAP* **0808** (2008) 002, [[arXiv:0805.4795](#)].
- [39] J. R. Bond, A. V. Frolov, Z. Huang, and L. Kofman, *Non-Gaussian Spikes from Chaotic Billiards in Inflation Preheating*, *Phys. Rev. Lett.* **103** (2009) 071301, [[arXiv:0903.3407](#)].
- [40] S. Mollerach, *Isocurvature baryon perturbations and inflation*, *Phys. Rev. D* **42** (Jul, 1990) 313–325.
- [41] A. D. Linde and V. F. Mukhanov, *Nongaussian isocurvature perturbations from inflation*, *Phys. Rev.* **D56** (1997) 535–539, [[astro-ph/9610219](#)].
- [42] K. Enqvist and M. S. Sloth, *Adiabatic CMB perturbations in pre big bang string cosmology*, *Nucl. Phys.* **B626** (2002) 395–409, [[hep-ph/0109214](#)].
- [43] D. H. Lyth and D. Wands, *Generating the curvature perturbation without an inflaton*, *Phys. Lett.* **B524** (2002) 5–14, [[hep-ph/0110002](#)].
- [44] T. Moroi and T. Takahashi, *Effects of cosmological moduli fields on cosmic microwave*

- background, *Phys. Lett.* **B522** (2001) 215–221, [[hep-ph/0110096](#)].
- [45] D. H. Lyth, C. Ungarelli, and D. Wands, *The primordial density perturbation in the curvaton scenario*, *Phys. Rev.* **D67** (2003) 023503, [[astro-ph/0208055](#)].
- [46] N. Bartolo, S. Matarrese, and A. Riotto, *On non-Gaussianity in the curvaton scenario*, *Phys. Rev.* **D69** (2004) 043503, [[hep-ph/0309033](#)].
- [47] C. Gordon and K. A. Malik, *WMAP, neutrino degeneracy and non-Gaussianity constraints on isocurvature perturbations in the curvaton model of inflation*, *Phys. Rev.* **D69** (2004) 063508, [[astro-ph/0311102](#)].
- [48] K. Enqvist and S. Nurmi, *Non-gaussianity in curvaton models with nearly quadratic potential*, *JCAP* **0510** (2005) 013, [[astro-ph/0508573](#)].
- [49] K. A. Malik and D. H. Lyth, *A numerical study of non-gaussianity in the curvaton scenario*, *JCAP* **0609** (2006) 008, [[astro-ph/0604387](#)].
- [50] M. Sasaki, J. Valiviita, and D. Wands, *Non-gaussianity of the primordial perturbation in the curvaton model*, *Phys. Rev.* **D74** (2006) 103003, [[astro-ph/0607627](#)].
- [51] J. Valiviita, M. Sasaki, and D. Wands, *Non-Gaussianity and constraints for the variance of perturbations in the curvaton model*, [astro-ph/0610001](#).
- [52] H. Assadullahi, J. Valiviita, and D. Wands, *Primordial non-Gaussianity from two curvaton decays*, *Phys. Rev.* **D76** (2007) 103003, [[arXiv:0708.0223](#)].
- [53] M. Bastero-Gil, V. Di Clemente, and S. F. King, *Preheating curvature perturbations with a coupled curvaton*, *Phys. Rev.* **D70** (2004) 023501, [[hep-ph/0311237](#)].
- [54] K. Enqvist, S. Nurmi, and G. I. Rigopoulos, *Parametric Decay of the Curvaton*, *JCAP* **0810** (2008) 013, [[arXiv:0807.0382](#)].
- [55] J. H. Traschen and R. H. Brandenberger, *Particle production during out-of-equilibrium phase transitions*, *Phys. Rev.* **D42** (1990) 2491–2504.
- [56] L. Kofman, A. D. Linde, and A. A. Starobinsky, *Reheating after inflation*, *Phys. Rev. Lett.* **73** (1994) 3195–3198, [[hep-th/9405187](#)].
- [57] L. Kofman, A. D. Linde, and A. A. Starobinsky, *Towards the theory of reheating after inflation*, *Phys. Rev.* **D56** (1997) 3258–3295, [[hep-ph/9704452](#)].
- [58] K. Dimopoulos, G. Lazarides, D. Lyth, and R. Ruiz de Austri, *Curvaton dynamics*, *Phys. Rev.* **D68** (2003) 123515, [[hep-ph/0308015](#)].
- [59] K. Enqvist, S. Nurmi, G. Rigopoulos, O. Taanila, and T. Takahashi, *The Subdominant Curvaton*, [arXiv:0906.3126](#).
- [60] M. Lemoine, J. Martin, and J. Yokoyama, *Constraints on moduli cosmology from the production of dark matter and baryon isocurvature fluctuations*, *Phys. Rev.* **D80** (2009) 123514, [[arXiv:0904.0126](#)].
- [61] A. A. Starobinsky, *Multicomponent de sitter (inflationary) stages and the generation of perturbations*, *JETP Lett.* **42** (1985) 152–155.
- [62] D. S. Salopek and J. R. Bond, *Nonlinear evolution of long wavelength metric fluctuations in inflationary models*, *Phys. Rev.* **D42** (1990) 3936–3962.
- [63] M. Sasaki and E. D. Stewart, *A general analytic formula for the spectral index of the density perturbations produced during inflation*, *Prog. Theor. Phys.* **95** (1996) 71–78, [[astro-ph/9507001](#)].
- [64] D. H. Lyth, K. A. Malik, and M. Sasaki, *A general proof of the conservation of the curvature perturbation*, *JCAP* **0505** (2005) 004, [[astro-ph/0411220](#)].
- [65] S. Y. Khlebnikov and I. I. Tkachev, *Classical decay of inflaton*, *Phys. Rev. Lett.* **77** (1996) 219–222, [[hep-ph/9603378](#)].
- [66] T. Prokopec and T. G. Roos, *Lattice study of classical inflaton decay*, *Phys. Rev.* **D55** (1997) 3768–3775, [[hep-ph/9610400](#)].
- [67] D. H. Lyth, *Can the curvaton paradigm accommodate a low inflation scale*, *Phys. Lett.* **B579** (2004) 239–244, [[hep-th/0308110](#)].
- [68] E. Komatsu and D. N. Spergel, *The cosmic microwave background bispectrum as a test of the*



- physics of inflation and probe of the astrophysics of the low-redshift universe*, astro-ph/0012197.
- [69] D. H. Lyth and Y. Rodriguez, *The inflationary prediction for primordial non-gaussianity*, *Phys. Rev. Lett.* **95** (2005) 121302, [astro-ph/0504045].
- [70] L. Senatore, K. M. Smith, and M. Zaldarriaga, *Non-Gaussianities in Single Field Inflation and their Optimal Limits from the WMAP 5-year Data*, arXiv:0905.3746.
- [71] P. B. Greene, L. Kofman, A. D. Linde, and A. A. Starobinsky, *Structure of resonance in preheating after inflation*, *Phys. Rev.* **D56** (1997) 6175–6192, [hep-ph/9705347].
- [72] G. N. Felder and I. Tkachev, *LATTICEASY: A program for lattice simulations of scalar fields in an expanding universe*, *Comput. Phys. Commun.* **178** (2008) [hep-ph/0011159].
- [73] A. Rajantie and E. J. Copeland, *Phase transitions from preheating in gauge theories*, *Phys. Rev. Lett.* **85** (2000) 916, [hep-ph/0003025].
- [74] A. Rajantie, P. M. Saffin, and E. J. Copeland, *Electroweak preheating on a lattice*, *Phys. Rev.* **D63** (2001) 123512, [hep-ph/0012097].
- [75] E. J. Copeland, S. Pascoli, and A. Rajantie, *Dynamics of tachyonic preheating after hybrid inflation*, *Phys. Rev.* **D65** (2002) 103517, [hep-ph/0202031].
- [76] D. I. Podolsky, G. N. Felder, L. Kofman, and M. Peloso, *Equation of state and beginning of thermalization after preheating*, *Phys. Rev.* **D73** (2006) 023501, [hep-ph/0507096].
- [77] M. Bastero-Gil, M. Tristram, J. F. Macias-Perez, and D. Santos, *Non-linear Preheating with Scalar Metric Perturbations*, *Phys. Rev.* **D77** (2008) 023520, [arXiv:0709.3510].